Article

Not peer-reviewed version

Anionic Hydrogels from Date Palm Waste for Dye Adsorption in Wastewater Treatment

Farid Fadhillah , Abdulrahman G. Alhamzani , Khaled Bin Bandar , Abdullah Alshamari , Saad Aljlil , Abdelrahman G. Gadallah , Mohamed Ahmed Habib , Mortaga M. Abou-Krisha , Mona A. Abdel-Fatah *

Posted Date: 23 May 2024

doi: 10.20944/preprints202405.1464.v1

Keywords: dye wastewater treatment; cellulose nanofiber; bio-adsorbent; palm date leaves; methylene blue

Article

Anionic Hydrogels from Date Palm Waste for Dye Adsorption in Wastewater Treatment

Farid Fadhillah [1], Abdulrahman G. Alhamzani [2], Khaled Bin Bandar [3], Abdullah Alshamari [3], Saad Aljlil [3], Abdelrahman G. Gadallah [1,4], M. A. Habib [2,5], Mortaga M. Abou-Krisha [2] and Mona A. Abdel-Fatah [4,*]

[1] Chemical Engineering Department, College of Engineering, Imam Mohammad Ibn Saud Islamic University (IMSIU), Riyadh, 11432, Saudi Arabia
[2] Department of Chemistry, Imam Mohammad Ibn Saud Islamic University, (IMSIU), Riyadh 11623, Saudi Arabia
[3] Water Management & Treatment Institute, King Abdulaziz City for Science and Technology (KACST), Riyadh, Saudi Arabia
[4] Chemical Engineering and Pilot Plant Department, Engineering and Renewable Energy Research Institute, National Research Centre, P.O. 12622 Dokki, Giza, Egypt
[5] Chemistry of Tanning Materials and Leather Technology Department, Chemical Industries Institute, National Research Centre, P.O. 12622 Dokki, Giza, Egypt
* Correspondence: monamamin7@yahoo.com

Abstract: This work aimed to develop an anionic cellulose nanofiber (CNF) bio-adsorbent from palm date tree waste and to investigate its removal efficiency against cationic methylene blue dye from contaminated water. Palm date pulp was first prepared from palm date leaves through acid hydrolysis using H_2SO_4, followed by hydrolysis in a basic medium using KOH, in which the process completely removed the components of hemicellulose, lignin, and silica. To obtain anionic CNF, the resulting pulp was further treated with H_2SO_4, followed by centrifugation. Biogel formation of the CNF suspension was promoted by sonication, where its removal efficiency of methylene blue dye was studied as a function of dye concentration, temperature, contact time, and pH value. In this work, we investigated two isotherms, i.e. Langmuir and Freundlich. The Langmuir model's consistency with the experimental data suggests that the adsorption of methylene blue dye onto CNF is monolayer and surface-limited. The reported maximum removal efficiency of 5 mg/g at 60°C indicates the optimal temperature for adsorption in this specific case. Additionally, pseudo-second order model and Elovich model were also utilized to obtain not only better understanding of adsorption mechanism in which not just physical adsorption but also the indication of chemical reaction occurring between methylene blue dye and CNF. The result showed that pseudo-second order model consistency with experimental data suggests that the adsorption of methylene blue (MB) onto CNF is rate-limiting step involving the chemisorption between the two. The study reveals that CNF adsorbents derived from renewable natural waste sources such as palm date leaves can be effective in removing cationic contaminants such as methylene blue dye.

Keywords: dye wastewater treatment; cellulose nanofiber; bio-adsorbent; palm date leaves; methylene blue

1. Introduction

The rapid development of varying industrial activities has created pressing environmental problems and prompted the urgent need to develop sustainable technologies to remediate these problems. In the case of water pollution problems, the use of natural sources for water treatments has gained a great deal of interest as these treatments can be sustainable and low cost. The existing pollutants in water from industrial activities are very diverse, including organic and inorganic particles, chemicals (e.g., detergents, pesticides, heavy metals, per- and polyfluoroalkyl substances (PFAS), and dyes), biomolecules (e.g., pharmaceuticals) and micro-plastics [1]. In addition to chemical pollution [2], natural pollution from events such as wind dust, emissions of volatile organic compounds from plants, and volcanic eruptions that can greatly alter the properties of water has also been recognized as notable environmental challenges [3].

 doi:10.20944/preprints202405.1464.v1

In this study, we aim to demonstrate a potentially low-cost material to remediate the contaminant problems involving azo dyes in textile, printing, and petroleum industries [1–5]. The common usage of azo dyes is because of their strong binding ability with the substrates (e.g., natural and synthetic fibers); such that the resulting colors would not be affected by light, washing, oxygen, acids, and bases [4]. The characteristic functionality of azo dyes [5] is the presence of n-n chromophoric group [6,7]. Among the different remediation techniques to remove azo dyes from water, the adsorption approach is considered the simplest and most energy-efficient approach [8], where its cost-efficiency can be greatly improved by the development of low-cost adsorption materials [9]. In the current study, methylene blue is chosen as a model azo dye, which has been found in large amount in many regions around the globe when the safe environmental practices are not strictly followed.

One promising candidate of low-cost adsorption materials is nanostructured bio-adsorbent derived from natural biomass sources, such as relatively underutilized agriculture residues, because they are abundant, sustainable and environmentally friendly [10,11]. Several bio-adsorbents have already been demonstrated for purification of polluted water resulting from paper industry [12], leather tanning [13,14], food processing, plastics, cosmetics, rubber, printing, and dye manufacturing industries [15–19]. Owing to its high adsorption capacity for a variety of pollutants in aqueous solutions, the utilization of activated carbon is widely acknowledged among bio-adsorbents [19]. The high adsorptivity is mainly due to the presence of heteroatoms like oxygen, nitrogen, and sulfur on the surface which enables adsorption interaction through various interactions such as hydrogen bonding, π-π interactions, and dipole-dipole interactions [20,21]. There are two fundamental mechanisms by which the substances adhere to the surface of an adsorbent namely, chemisorption and physisorption. Chemisorption involves the formation of strong chemical bonds between the adsorbate and the adsorbent. The chemical bonds formed in chemisorption are often difficult to break, making the process largely irreversible under normal conditions. In contrast, physisorption is characterized by weaker interactions, such as van der Waals forces. Due to its weaker interaction, physical adsorption is often reversible, allowing the adsorbate to be easily desorbed from the adsorbent surface under appropriate conditions.

The adsorption ability of bio-adsorbents derived from agricultural residues can contain both physical and chemical adsorptive interactions (if the adsorbent surface is ionically charged). The main physical interactions involve van der Waals forces, hydrogen bonds, polar interactions, Π-Π interaction, etc. The conversion of natural biomass feedstocks into effective bio-adsorbents requires proper treatments. For production of activated carbon, the approach usually involves the use of pyrolysis to treat dense biomass feedstock (e.g. coconut shell and wood), followed by an activation step [22]. However, such an approach is generally not economically beneficial to treat porous biomass feedstock (i.e. leaves, agricultural stalks…). As all plant-based biomass feedstocks contains linear cellulose polymers with β-1,4-linked D-glucose repeating units, the recent treatments to produce anionic CNF will be appropriate to produce a different kind of bio-adsorbent with abundant hydroxyl (and other functional) groups that can create intermolecular and intramolecular interactions to remove contaminants [23]. These adsorbents are typically in the suspension state, and thus can be used more as coagulants/flocculants instead of solid adsorbents (e.g., activated carbon) for water purification.

The biomass feedstocks most suitable for low energy anionic CNF production include leaves, grasses, natural fibers, and marine algae [24]. This is because these feedstocks have relatively loose structure, high porosity and low lignin content, where high surface area can be produced in even mild defibrillation conditions, yielding high adsorption efficiency. These are several interesting examples in the literature using agricultural biomass for dye removal. For example, the performance of several cellulose-based aerogels prepared from Pomelo fruit to adsorb different dyes (i.e., methylene blue, malachite green, rhodamine 6G, rose bengal, and methyl orange) have been studied. These aerogels include cellulose (CA), graphene oxide (GOA), and cellulose-graphene oxide composite (CGA). It was found that the adsorption efficiency of CGA aerogels (98%) against methylene blue dyes is higher than those of GOA (95%) and CA (74%) aerogels [25]. The adsorption

 doi:10.20944/preprints202405.1464.v1

of methylene blue dye in an aqueous solution using a polyester nonwoven modified by cross-linked carboxymethyl cellulose and synthesized ZIF-8 has also been investigated [26].

The study involved the change of dye concentration and contact time in both batch and continuous fixed bed conditions. The result showed that there is slight variation in performance between continuous and batch systems. For continuous system, the adsorption capacity of 0.824 mg/g was observed whereas for batch system, it was found to be 0.829 mg/g. Both results were obtained at initial concentration ranging from 2 to 8 mg/l. With increasing initial dye concentration from 2 to 8 mg/l, the adsorption capacity was increased about 80 and 90% in batch and continuous systems, respectively. In another example, regenerated cellulose (RC) has been used as an adsorbent for wastewater streams containing varying dyes. The RC adsorbent was produced by the cellulose dissolution waste stream, where the maximum adsorption capacity of RC against crystal violet was 398.41mg.g^{-1} and its maximum adsorption capacity against methylene blue was 367.65mg.g^{-1} [27]. Finally, hydrogel with an average particle size of around 14.9 μm was synthesized from carboxymethyl cellulose nanocrystals and L-cystenine, where the composite hydrogel was used as an adsorbent for methylene blue removal. The maximum adsorption capacity of this hydrogel system could reach 756 mg/gm at pH ≈11 [28].

In this study, we aimed to demonstrate the production of cellulose nanofibers using a typical method from renewable natural resources such as palm date leaflets, which are abundant in the local environment but often considered as waste. The resulting anionic CNF was tested as a bio-adsorbent for dye removal using MB as a model dye contaminant. The optimal condition for the maximum removal efficiency was evaluated and compared with other bio-adsorbents. The broader impact of this study includes the waste upcycling and sustainable remediation materials development to tackle industrial water pollution challenges.

2. Experimental

2.1. Materials

Palm tree leaflets, as a renewable cellulose-rich material, were collected from a local farm in our region. MB dye was supplied by the Aldrich Chemical Company, USA. Sodium hydroxide (NaOH); potassium hydroxide (KOH); sulphuric acid (H_2SO_4); acetic acid (CH_3COOH); and sodium chlorite ($NaClO_2$) were high-grade laboratory chemicals, purchased from BDH Chemicals. All chemicals were used as received without further purification.

2.2. Preparation of Cellulose

A detailed and methodical approach to the preparation of cellulose pulp from palm date leaflets is explained in this section. This procedure involves several critical steps that ensure the removal of non-cellulosic components such as hemicellulose, lignin, and silica, which are typical in lignocellulosic biomass. Initially, the palm date leaflets are thoroughly washed with distilled water to remove dust and impurities and followed with one day air-dried. They are subsequently cut and ground into smaller pieces, followed by milling to achieve a uniform size of less than 5mm. The ground fibers are then treated with sulfuric acid under reflux conditions, which helps in hydrolyzing and removing hemicellulose. In this step, 150g of ground leaflet fiber was mixed in a 1-liter round-bottom flask, where 40g of sulfuric acid was added gradually under reflux for 2h at 90^{o}C. The mixture is then filtered and washed using deionized water until a neutral pH is achieved.

After the removal of hemicellulose, an alkaline hydrolysis step is executed employing 20% of KOH solution to break down and remove lignin and silica. This process also involves refluxing, filtration, and thorough washing to reach a neutral pH. A liquid-solid ratio of 10:1 at the same refluxing temperature and time (90^{o}C for 2h) was used. The next step is bleaching of the cellulose pulp using a $NaClO_2$ solution at an acidic pH adjusted with acetic acid, which helps in removing the remaining lignin and amorphous cellulose. The solution is stirred at 75°C for 4 hours. Finally, the bleached pulp is filtered, washed to neutrality, and dried in an oven at 80°C until a constant weight is obtained, indicating the removal of all moisture.

 doi:10.20944/preprints202405.1464.v1

2.3. Preparation of Anionic Cellulose Nanofiber (CNF)

To ensure the production of high-quality CNF, we hydrolyzed never-dried cellulose pulp under controlled acidic conditions, followed by several purification and homogenization steps. Here is the procedure. Initially, the cellulose pulp was hydrolyzed with a 60wt% H_2SO_4 solution at a liquid-to-solid ratio of 1:10. The acid solution was added slowly to the cellulose suspension, and the reaction was conducted at a temperature of 45°C for 60 minutes. The hydrolyzed product was extensively washed with cold deionized water to remove any residual sulfuric acid. This was done by centrifuging the mixture at 5,000 rpm for 20 minutes, repeated seven times. The washed suspension was then placed into dialysis tubes with a molecular weight cut-off (MWCO) of 6-8 kDa and dialyzed against deionized water for 48 hours to equilibrate to a neutral pH of 6.7-6.9. To ensure homogeneous dispersion of the CNF suspension, the hydrolyzed product was sonicated at a frequency of 20 kHz for 10 minutes at a temperature of 10°C. The ratio of the suspension to water was maintained at 20:1. The sonicated suspension was then centrifuged at 10,000 rpm for 10 minutes to collect the CNF and followed with drying in the an oven at 60°C for 2 hours. The dried CNF was finally stored in sealed containers to prevent contamination and moisture uptake.

2.4. CNF Characterization

The scanning electron microscopic (SEM) imaging on the prepared cellulose and CNF samples using of was done using JSM-IT 500 HR (JEOL, Japan) instrument operated at an accelerating voltage of 10 kV. Prior to SEM, the samples were mounted on metal holders and sputter-coated with a thin layer of gold. The coating was applied for 45 minutes to enhance the electrical conductivity of the sample surface, which is essential for SEM imaging to prevent charging effects and obtain high-quality images.

The X-ray diffraction (XRD) of the different samples was investigated utilizing D8 Brucker X-ray diffractometer, with the Cu-Kα radiation with a wavelength (λ) of 1.54178 Å and operated over a 2θ range of 10-70 degrees with a step size of 0.02 degrees. XRD patterns were collected for the raw material, cellulose pulp, and CNF to investigate their crystalline structures and to identify any changes in crystallinity due to the treatment and processing of the samples.

Corresponding Fourier transfer infrared (FTIR) spectroscopy of different samples (the raw material, cellulose and CNF) was carried out using a Nicolet 6700 instrument in the transmission mode, where the FTIR spectra were recorded between 4500 and 400 cm^{-1} with a spectral resolution of 4 cm^{-1}.

2.5. Dye Adsorption Study

Before the dye adsorption study using bio-adsorbents, the following light adsorption measurement was first carried out. A spectrophotometer (Spectronicgenesys 5, model 336008, U.S.A) was used to determine the maximum wavelength at which the highest dye absorption efficiency occurred (the max. wavelength was 664 nm for MB). For determining the sensitivity range of the spectrophotometer in measuring the absorbance of MB dye, a calibration curve was first established. The absorbance of MB dye concentrations was measured in the range of 1- 4 ppm at the maximum wavelength of 664 nm. Following Beer's law, a linear relationship between the absorbance and the dye concentration was obtained Figure 1, which allowed the determination of MB dye concentration between 1 to 7 mg/l. For higher concentrations, the tested solutions were diluted accordingly.

 doi:10.20944/preprints202405.1464.v1

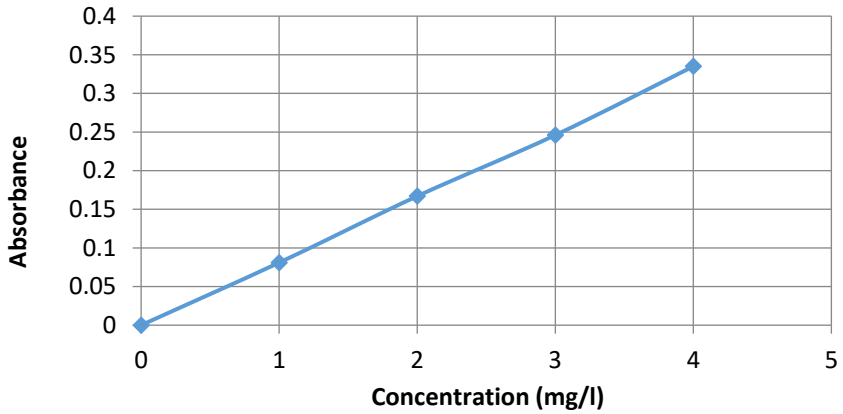

Figure 1. Calibration curve of MB dye.

2.6. Experimental Adsorption Equilibrium Isotherm

The adsorption experiments to evaluate the dye removal efficiency of CNF adsorbents were carried out in a 250ml stoppered conical flask containing 50ml of dye solution at varying concentrations. The adsorption equilibrium isotherm data were obtained from the batch adsorption experiments at an agitation speed 250 rpm. The initial dye concentration was prepared by diluting a stock solution with a known concentration of 1000 mg/L. To calculate the amount of dye adsorbed at equilibrium per unit mass of the adsorbent, the following equation is used

$$q_e = V\frac{(C_o - C_e)}{m} \quad (1)$$

Where: , V (l) is the volume of solution, m (g) is the mass of the adsorbent used C_o and C_e ($mg.l^{-1}$) are the initial and final concentrations of dye in the aqueous solution, respectively.

There are several experimental factors such as pH of the solution, the initial concentration of the dye, and contact Time. pH influences both the surface charge of the adsorbent and the ionization state of the dye molecules thus it can significantly affect the adsorption process. By varying the initial concentration of the dye, the adsorbtion capacity of the CNF at different concentrations can be studied. Meanwhile, duration of the interaction between the dye solution and the CNF can determine how quickly equilibrium is reached and the efficiency of adsorption over time. Figure 2 presents the equilibrium between the amount of adsorbed MB on the CNF and concentration of MB in the solution.

 doi:10.20944/preprints202405.1464.v1

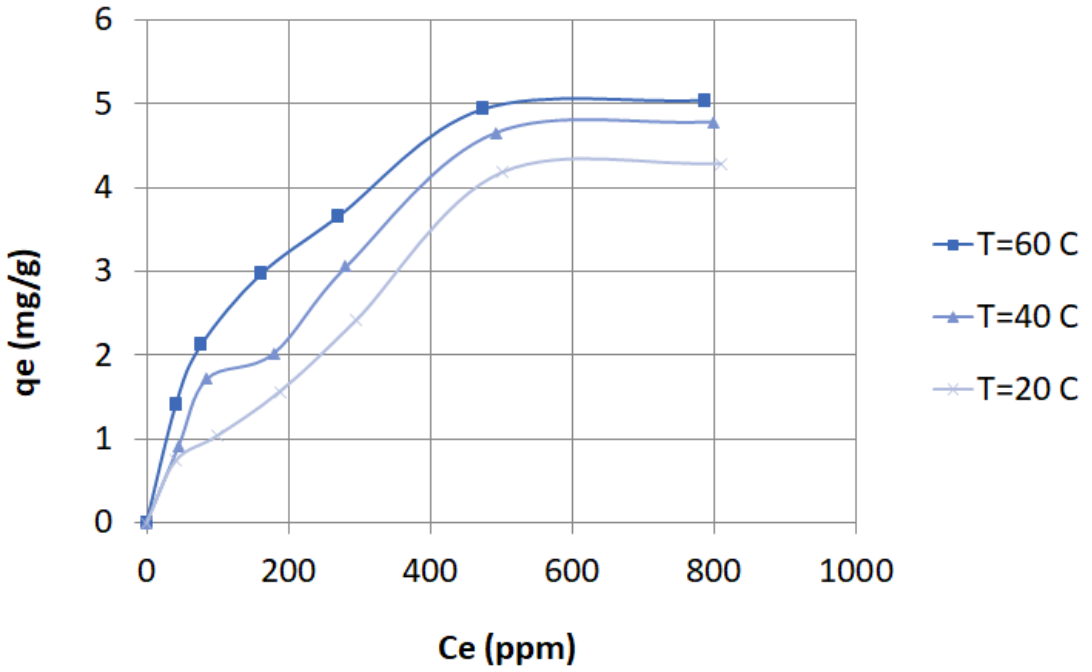

Figure 2. Adsorption of MB on anionic CNF at different temperatures.

2.7. Kinetic Experiments

It is important to measure the adsorption rate precisely during the kinetics experiments. The below procedure was methodically structured to evaluate the influence of agitation speed and initial MB concentration on the adsorption kinetics. To initiate the adsorption process, 1 gram of anionic CNF is added to 50 ml of the MB solution. Initial concentrations of MB are prepared and placed into special bottles. These bottles are then situated in a thermostat-controlled shaker to ensure a constant temperature throughout the experiment, which is crucial for maintaining consistent experimental conditions. The adsorption process is monitored over a period of 90 minutes. During this time, the agitation speed is controlled and maintained at a specific rate. Typically, the adsorption rate is higher at the beginning due to the abundance of available adsorption sites and decreases gradually as these sites are occupied, until equilibrium is reached where no further adsorption occurs. At predetermined time intervals during the 90-minute shaking period, samples are taken from the shaker. These samples are immediately filtered to separate the CNF from the MB solution to measure the remaining amount of MB.

The agitation speed plays an important role in the adsorption process. The agitation is needed to mix the solution which in turn affects the mass transfer of the adsorbate to the adsorbent. In our work, the procedure that was previously explained was done for various agitation speeds and initial MB concentrations. The adsorption experiments were conducted with agitation speeds set at 100 rpm, 200 rpm, and 250 rpm. These speeds were chosen to represent a range of mixing intensities that could influence the mass transfer rate of MB to the anionic CNF. The resulting data of concentration against time was plotted as shown in Figure 3. Meanwhile, to assess the effect of initial MB concentration on the adsorption process, concentrations varied from 100 ppm to 600 ppm. During these experiments, the agitation speed was consistently maintained at 200 rpm, ensuring that the only variable affecting the adsorption rate was the initial concentration of MB. Similarly, the resulting data of concentration against time was also plotted as shown in Figure 4.

Preprints.org (www.preprints.org) | NOT PEER-REVIEWED | Posted: 23 May 2024 doi:10.20944/preprints202405.1464.v1

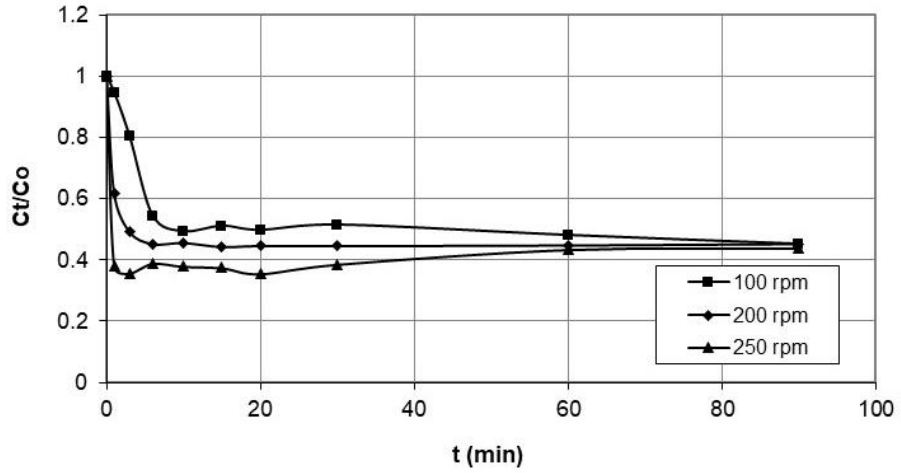

Figure 3. Adsorption rate of MB on anionic CNF at C_o= 100 ppm and varying stirrer speeds.

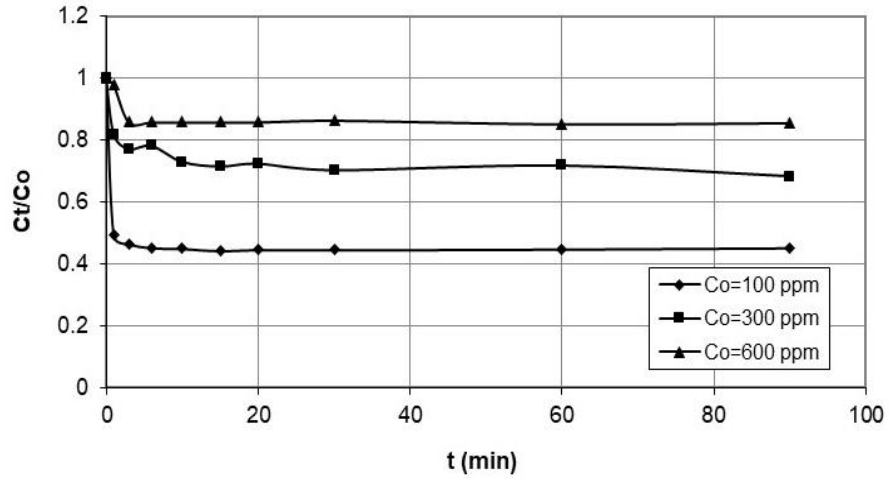

Figure 4. Adsorption rate of MB on anionic CNF (at 200 rpm and varying initial concentrations).

2.8. Adsorption Equilibrium Isotherm Models

The Langmuir & Freundlich isotherms are two commonly employed models for characterizing the adsorption process of contaminants such as dyes on various adsorbents.

2.8.1. Langmuir Isotherm Model

The Langmuir isotherm model is based on the assumption that adsorption occurs at specific homogeneous sites within the adsorbent and that once a dye molecule occupies a site, no further adsorption can take place at that site. The relation is expressed as follows:

$$q_e = \frac{K\,C_e}{1+bC_e} \qquad (2)$$

The model can be linearized as follow:

$$\frac{C_e}{q_e} = \frac{1}{K} + \left(\frac{b}{K}\right) C_e \qquad (3)$$

Hence, a plot of C_e/q_e versus C_e provides the equilibrium-constant K and b, for the adsorption process obtained from the slope and intercept of the linear plot.

2.8.2. Freundlich Isotherm Model

The Freundlich isotherm model, on the other hand, assumes a heterogeneous surface with a non-uniform distribution of heat of adsorption over the surface. The Freundlich isotherm is an empirical equation that can be represented as:

 doi:10.20944/preprints202405.1464.v1

$q_e = K_F\ C_e^{1/n}$ (4)

The linearization of Freundlich model is expressed as follows:

$\log q_e = \log K_F + \left(\frac{1}{n}\right) \log C_e$ (5)

The constants, K_F and n are obtained from the intercept and slope of linear plot log q_e against log C_e.

To validate experimental results, one would typically fit the experimental data to both the Langmuir and Freundlich isotherm models and determine the corresponding parameters for each model. The goodness of fit is often assessed using statistical metrics such as the coefficient of determination (R^2) or the chi-square test. The model that best describes the adsorption process is determined by the higher correlation coefficients and the conformity of the model assumptions with the experimental observations.

2.9. Kinetic Models

Kinetic models including those in which chemical reaction is considered as the rate limiting step are also used to explain the experimental data.

2.9.1. Describing the Batch Adsorption Process Using Reaction Models

Many researchers used pseudo-first order, pseudo-second order and Elovich model to study dyes-adsorption that involves chemical reactions as the rate limiting step [29–39].

Pseudo-First-Order Model

In the case of pseudo-first order model, the adsorption rate of MB on CNF is assumed to be proportional to the amount of adsorbed MB. The model is expressed as follows:

$$\left(\frac{dq_t}{dt}\right) = k_1 (q_e - q_t) \quad (6)$$

Where: q_e and q_t are the adsorption capacities (mg/g) of MB at equilibrium and time t, respectively. Whereas, k_1 is the pseudo-first-order adsorption-rate constant (1/min). by integrating equation (6) and using initial condition $q_t = 0$ at $t = 0$, one can obtain:

$ln\ (q_e - q_t) = ln\ q_e - k_1\ t$ (7)

Here, q_t can be found using the following method:

$q_t = \frac{V(C_0 - C_t)}{M}$ (8)

In addition, q_e can be calculated as follows:

$q_e = \frac{V(C_0 - C_e)}{M}$ (9)

Where:

C_o = initial concentration of methylene blue (mg/L)

C_t = concentration of methylene blue at time t (mg/L);

C_e = concentration of methylene blue at equilibrium (mg/L).

Pseudo-Second-Order Model

MB adsorption can also be described using modified second order pseudo equation. It can be written as:

$\frac{dq_t}{dt} = k_2(q_e - q_t)^2$ (10)

Where: q_e and q_t are the adsorption capacities (mg/g) of MB at equilibrium and time t, respectively. Meanwhile k_2 (g/mg·min) is pseudo-second-order adsorption-rate constant. Equation (10) can be integrated, using the boundary condition of $q_t = 0$ at $t = 0$ and $q_t = q_t$ at $t = t$, one can obtain the following equation:

Preprints.org (www.preprints.org) | NOT PEER-REVIEWED | Posted: 23 May 2024 doi:10.20944/preprints202405.1464.v1

$$\left(\frac{t}{q_t}\right) = \left(\frac{1}{k_2 q_e^2}\right) + \left(\frac{1}{q_e}\right) t \qquad (11)$$

As shown, if the data fits the model, one can obtain linear relationship with a slope of $1/q_e$ and an intercept of $(1/k_2 q_e^2)$ by plotting (t/q_t) versus t.

Elovich Model

The Elovich equation is expressed as follows:

$$\left(\frac{dq_t}{dt}\right) = œ \exp(-ß\, q_t) \qquad (12)$$

Where: it is the methylene blue amount adsorbed on anionic CNF at time t, œ is the initial MB adsorption rate (mg/g·min), and ß is the desorption constant (g/mg) for a given experiment period. For the simplification of the Elovich equation, assuming ß >> 1, the boundary condition $q_t = 0$ is applied when t= 0, and $q_t = q_t$ is applied when t= t, then Equation (12) becomes:

$$q_t = ß \ln(œ\, ß) + ß \ln t \qquad (13)$$

To determine the Elovich equations that fit the kinetics, Equation (13) was used to represent the adsorption rate of methylene blue on anionic CNF. Thereafter, constant values can be obtained from the linear slope and intercept of the plot of q_t versus ln t.

3. Results and Discussion

3.1. Characterization of Anionic CNF

The change in the raw material structure resulting from the chemical and thermal treatment was studied using electron microscopy imaging Figure 5. From the images,

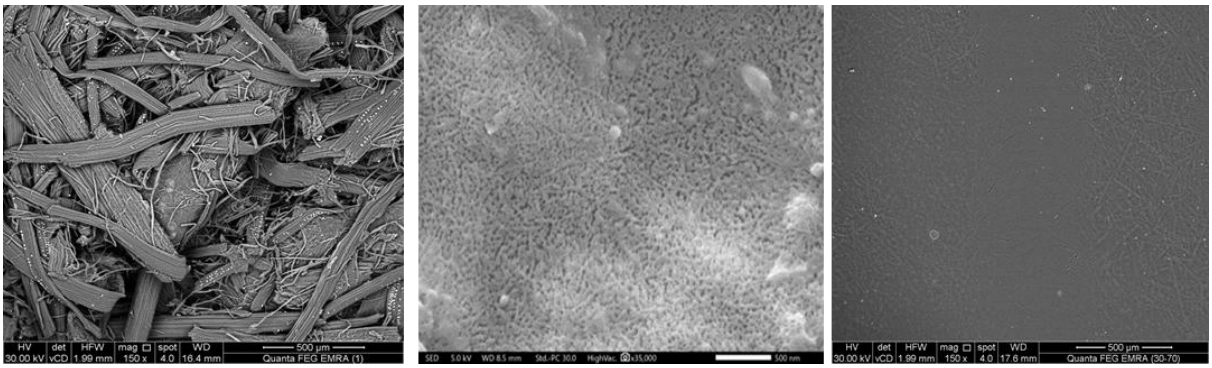

(a) **(b)** **(c)**

Figure 5. (a) SEM images of hydrolyzed cellulose - (b), and (c) SEM images of prepared anionic CNF.

The change in the ratio between the amorphous and crystalline forms during the chemical and thermal treatment process was studied by X-ray spectrometry. It is well known that natural cellulose is cellulose I. It converts to cellulose II under the effect of an alkaline treatment. Knowing that cellulose 'I' is metastable and cellulose 'II' is stable, it is possible to form cellulose III and cellulose IV with the progress in the alkaline treatment. The transformation of cellulose I to cellulose II can be investigated by x-ray. The XRD diffraction of the cellulose has been recorded at the different characteristic peaks 2θ Figure 6 that are corresponding to the lattice crystal. It can be seen that the fibers of palm tree leaflet are soft and long, and they have a smooth surface Figure 5a.

 doi:10.20944/preprints202405.1464.v1

Also, the SEM images Figure 5b confirm that the fibers have become shorter in length and their width has been reduced as a result of the cooking or hydrolysis process, where lignin and minerals are removed. It can also be noted that the radius of the fibers is up to 30 microns, and that the size decreases with progress in hydrolysis processes until it reaches a size of less than 60 nanometers with a highly homogeneous shape. The presence of the characteristic two peaks around ($2\theta = 22.6^{o}$ and 16^{o}) indicates the cellulose nano-structure [40].

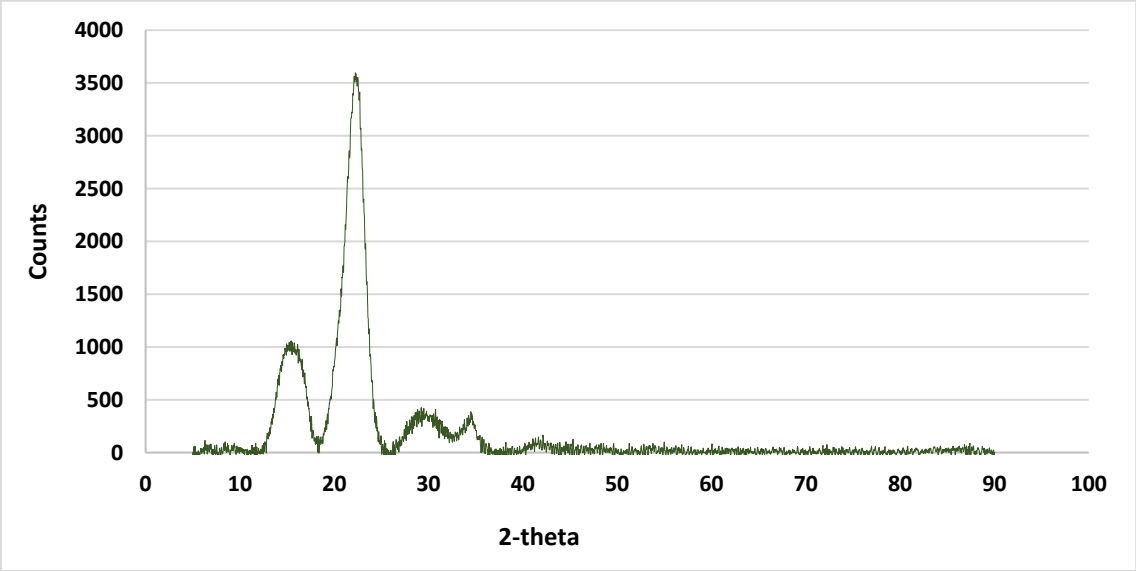

Figure 6. XRD pattern of the Nano cellulose fiber.

The degree of crystallinity was calculated according to the following equations.

$$CI(\%) = \frac{Acrystalinity}{Aamorphous+Acrystalinity} x\ 100 \qquad (14)$$

Where: $A_{amorphous}$ represents the area under the curve of the amorphous, $A_{crystalline}$ is the area under the curve of the sample.

The Crystal size:

$$L = \lambda k / c\ \beta\ \theta \qquad (15)$$

Where: λ=0.1540 nm, k represents the correction factor of 0.91, θ represents diffraction angle in radians and β represents full width at half maximum

The FTIR analysis shown in Figure 7 provides valuable information regarding the chemical composition and functional groups present in the raw material, extracted cellulose, and CNF. The broad spectral band in the range of 3630-3105 cm^{-1} is indicative of O-H stretching vibrations, which are typically associated with the hydroxyl groups present in the cellulose and other polysaccharides [41]. The peak observed at the wavenumber of 1692 cm^{-1} is attributed to C=C stretching vibrations, which are characteristic of aromatic structures found in lignin. The absorption peak at 1160 cm^{-1} is associated with C–O–C asymmetric stretching vibrations. This peak is characteristic of the glycosidic linkages between sugar units in cellulose, hemicellulose, and lignin. It confirms the presence of these polysaccharides in the samples and is a strong indication of the polysaccharide backbone structure [42,43].

 doi:10.20944/preprints202405.1464.v1

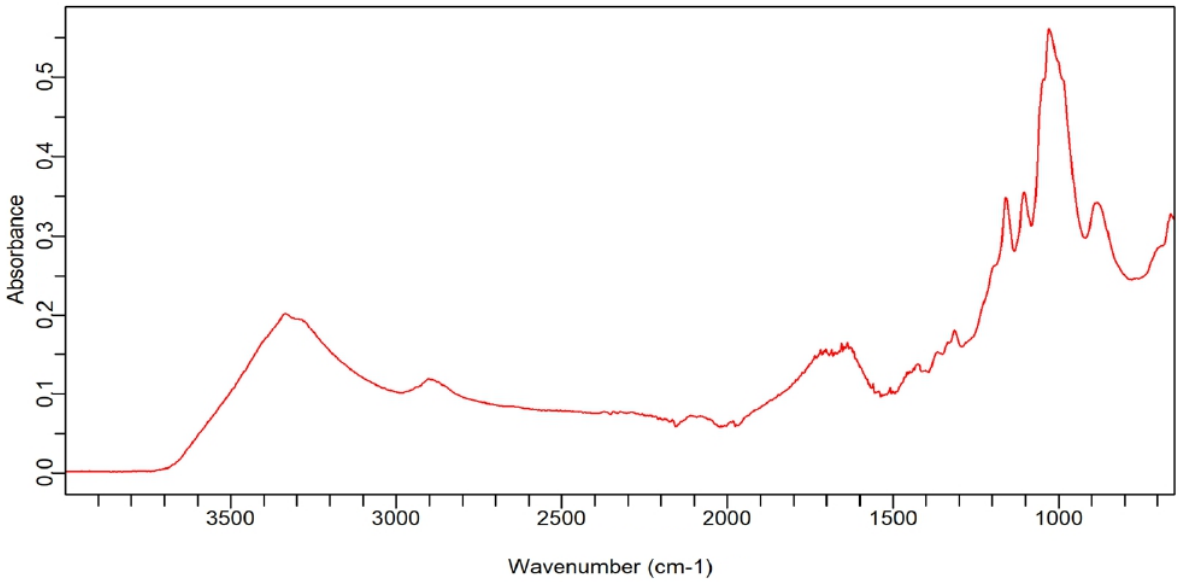

Figure 7. FTIR spectra of anionic CNF.

It is clear from Figure 8 that the sample is a gel-like suspended solution, which confirms the obtaining of the characteristic gel generation of nanomaterial.

Figure 8. Sample of the obtained nano-cellulose.

3.2. Equilibrium Time Experiments

To ascertain the equilibrium time, Figures 3–4 indicate that it takes 40 minutes for the dye/anionic CNF to reach equilibrium.

3.3. The Effect of pH

The observation of the effect of the pH on removal efficiency was investigated in the range 2 and 12. The use of 0.5 M NaOH and 0.5 M HCl is a frequent practice to adjust the pH value. It is apparent from the data shown in the Figure 9 that the adsorption efficiency of the anionic CNF for the positively charged dye increases with pH from 3 to 5. The maximum dye uptake has been recognized at pH of 6. This phenomenon is due to enhanced electrostatic attractions at this pH level.

 doi:10.20944/preprints202405.1464.v1

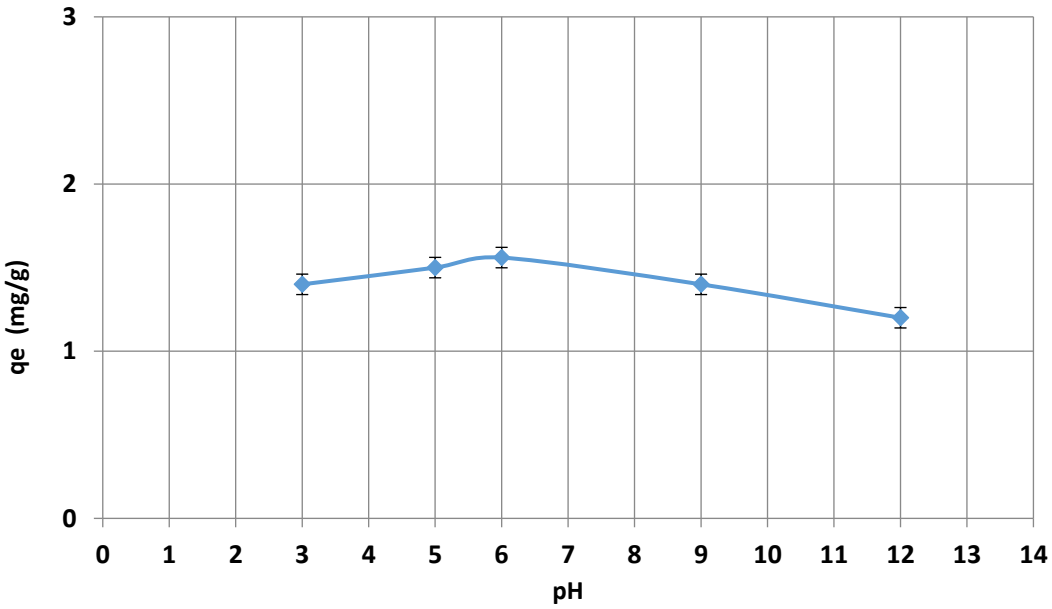

Figure 9. pH vs. q_e for adsorption of dye on anionic CNF.

3.4. The Effect of the Dye Equilibrium Constant

Understanding adsorption characteristics is crucial for optimizing the use of the nanomaterial in practical applications. For that purpose, we studied the equilibrium adsorption isotherm which is a graphical representation that plots the amount of dye adsorbed (often expressed in mg of dye per g of adsorbent) against the equilibrium concentration of the dye in the solution. We investigated the isotherm at various temperatures (20°C, 30°C, and 40°C). The result showed that the maximum adsorption capacity of the dye on the surface of the anionic CNF was found to be 4.25 mg/g at 20°C.

3.5. The Effect of Temperature

The impact of temperature on the adsorption was examined at temperatures ranging from 20°C to 60°C. The Data in Figure 2 shows that the adsorption capacities increase at higher temperatures. Since the adsorption process is exothermic. Increasing the temperature of the adsorption of dye on CNF is favorable. In this work, the maximum dye removal has been recognized at 5 mg/g.

3.6. The Adsorption Mechanism

The variation of the zeta potential of the anionic CNF concerning pH has been studied to determine the surface charge of the adsorbent. The results of variable zeta potential as a function of pH are shown in Figure 10. The dye adsorption on anionic CNF is influenced by the pH of the solution. The charge on the surface of the anionic CNF varied with the pH change, which results in variations in removal efficiency. The negative charges at the surface of the anionic CNF increase at higher pH value, therefore the molecules of the cationic dye will be more attractable to surface; accordingly the dye removal efficiency will be enhanced.

 doi:10.20944/preprints202405.1464.v1

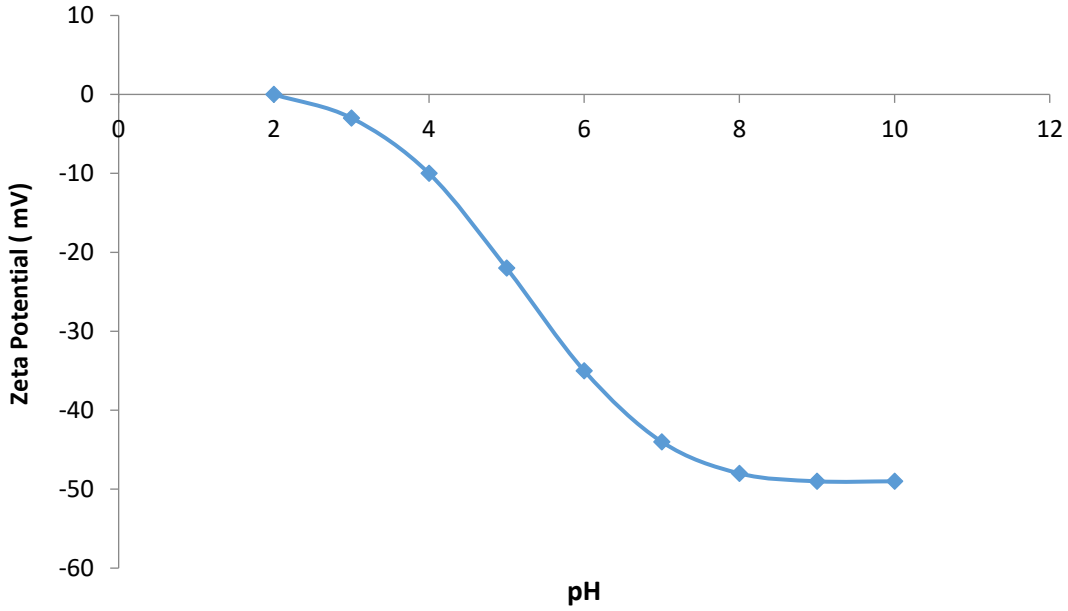

Figure 10. Variation of zeta potential versus pH for adsorption of dye on anionic CNF.

3.7. Adsorption-Equilibrium Isotherm

The resulting data showing the equilibrium-adsorption isotherm is plotted in Figure 2. The isotherm illustrates the relationship between the amount of adsorbed MB on CNF and the equilibrium MB concentration in the solution under the experimental conditions. That the maximum adsorption capacity of MB on anionic CNF is founds to be 4.25 mg/g at 20°C. This result suggests a strong interaction between the dye molecules and the surface of the nanofibers at this temperature.

The use of equilibrium adsorption isotherms, such as the Langmuir and Freundlich models, to analyze the adsorption process is a well-established method. The determination of the Langmuir isotherm constants (K and b) and the Freundlich isotherm constants (KF and n) through the linearized plots provides a quantitative measure of the adsorption process. For instance, plotting the Ce/qe versus Ce using linearized Langmuir model, shown in Figure 11), allows the determination of the equilibrium-constant parameters for the adsorption process based on the calculated slope and intercept. The Langmuir equilibrium parameters, K and b, of the system were listed in Table 1. The result suggests that Langmuir model satisfactorily explained the experimental data According to the value of the adjusted coefficient of determination R^2, the Langmuir model sufficiently explained the experimental data.

Table 1. Isotherm constants for MB adsorption on anionic CNF.

	Langmuir Isotherm			**Freundlich Isotherm**		
Temperature (°C)	**K (l/g)**	**b (l/mg)**	**R^2**	**k_F (l/g)**	**n (-)**	**R^2**
20	0.014	0.002	0.825	0.058	1.529	0.943
40	0.022	0.003	0.94	0.109	1.716	0.959
60	0.041	0.007	0.992	0.295	2.254	0.972

Preprints.org (www.preprints.org) | NOT PEER-REVIEWED | Posted: 23 May 2024 doi:10.20944/preprints202405.1464.v1

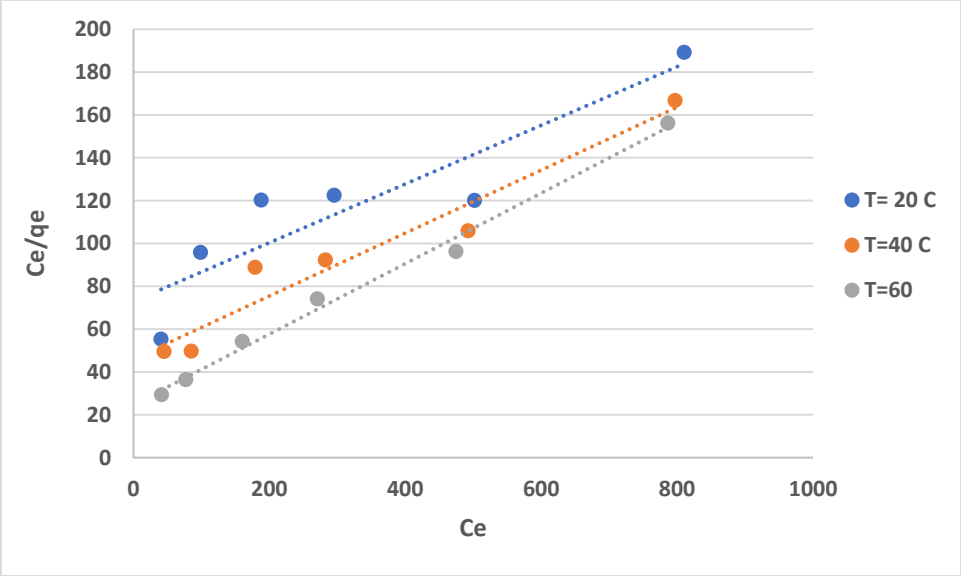

Figure 11. Langmuir isotherm fitting the experimental data of MB adsorption onto anionic CNF.

Similarly, Freundlich isotherm was also used to study the adsorption mechanism and all its equilibrium-constant parameters, i.e. KF and n, was obtained from the slope and intercept of linearized Freundlich model. Figure 12 shows that Freundlich model better fits the experimental data rather than Langmuir model. It is also supported by comparing R^2 value shown in Table 1. However, the observation on both isotherms is intriguing as the Langmuir model fits the experimental data better at higher temperatures, while the Freundlich model provides a better fit at lower temperatures. This could suggest that the adsorption mechanism of MB onto anionic CNF may transition from a monolayer adsorption process (Langmuir) at higher temperatures to a multilayer or heterogeneous adsorption process (Freundlich) at lower temperatures. Another observation was the value of n that is greater than unity indicates MB is readily adsorbed on anionic CNF [44].

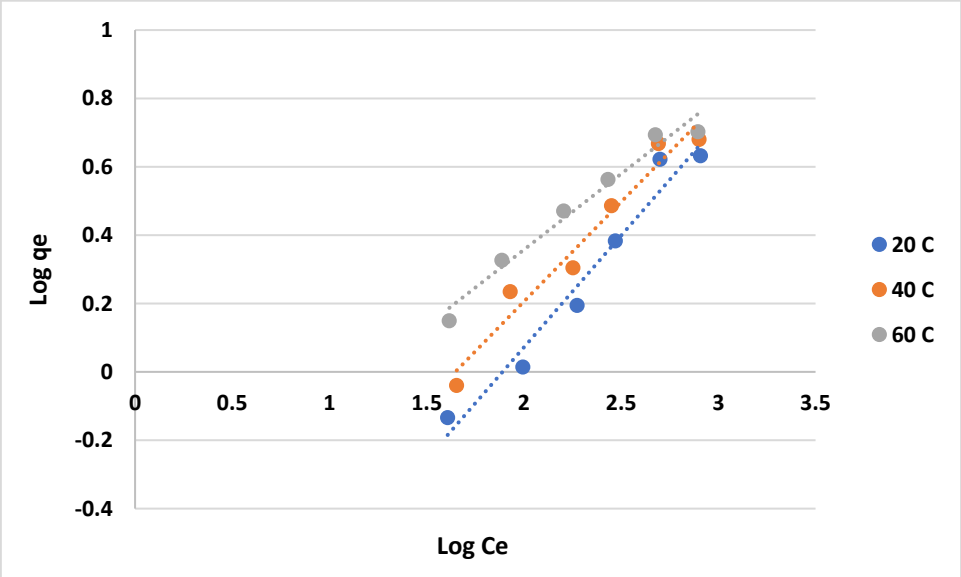

Figure 12. Freundlich isotherm fitting the experimental data of MB adsorption onto anionic CNF.

3.8. Kinetic Studies

As shown in Figures 3–4, the amount of MB in the wastewater gradually decreases due to it are binding to anionic CNF surface. The initial concentration of methylene blue in the wastewater is one of the factors influencing the adsorption of MB onto the anionic CNF from wastewater. In general,

 doi:10.20944/preprints202405.1464.v1

the lower initial concentrations of MB show more quickly concentration decrease than the higher initial concentrations. This is because at lower initial MB concentration, less binding sites are occupied by MB molecules thus there are more remaining vacant binding sites available for the adsorption. This results in higher rate of adsorption. Because of this higher rate of adsorption, the concentration of MB drops quickly [45]. Agitation plays a crucial role in the kinetics of adsorption by influencing the mass transfer of MB on the anionic CNF. At higher agitation speeds, the increased turbulence within the solution reduces the boundary layer thickness around the adsorbent particles, enhancing the mass transfer rate. Thus, the MB concentration decreases more quickly. On the other hand, mass transfer may end up being the rate-limiting step in the adsorption process at low agitation speeds due to thicker boundary layer around the adsorbent providing more resistance on transfer process [46].

3.8.1. Discussion of the Effect of the Chemical-Reaction as "a Rate Controlling Step" Using "Reaction Models" to Describe the Chemical Reaction Mechanism

The use of various kinetic models, such as the "pseudo-first-order", "pseudo-second-order", and "Elovich models", is a robust approach to further reveal and explain the adsorption mechanism which may include chemical reaction. The results showed that the agitation speed and the initial MB concentration also significantly affect the adsorption rate.

The data shown in Figures 13–14 represent the results for various initial concentrations and agitation speeds for the pseudo-first-order model. Whereas Table 2 list of the corresponding parameters. The correlation coefficient (R^2-value) suggests very poor fitting between the model and the experimental data. Meanwhile, the data presented in Figures 15–16, show the results for "pseudo second-order model". The R^2-value for this model is presented in Table 2 suggesting that the model accurately represents the experimental data. The Pseudo second-order model exhibits even better fitting compared to Elovich model (see Figure 17–18). In general, it is clear that both the "pseudo-second-order" model and the Elovich equation have been found to be more suitable for representing the experimental results, as opposed to the "pseudo-first-order model". Thus, chemisorption could be the mechanism of adsorption occurs in the adsorption of MB using CNF [47].

Table 2. Kinetic models parameters for MB adsorption on anionic CNF.

Adsorbent parameters	**Pseudo-first-order**		**Pseudo-second-order**		**Elovich**		
	k_1 (min^{-1})	**R^2**	**k_2 (g/mg. min)**	**R^2**	**œ (mg/g. min)**	**ß(g/mg)**	**R^2**
Initial conc. (mg/l)							
100	-0.001	0.119	17.63	0.921	21.56	0.089	0.597
300	-0.003	0.558	0.0748	0.894	0.049	0.4891	0.874
600	-0.0009	0.12	0.232	0.998	5.3e-05	0.560	0.463
Agitation speed (rpm)							
100	-0.0009	0.347	2.697	0.956	0.112	1.124	0.765
200	-0.002	0.151	2.749	0.955	4.417	1.529	0.634
250	-0.0011	0.425	2.695	0.955	11.14	2.445	0.760

Preprints.org (www.preprints.org) | NOT PEER-REVIEWED | Posted: 23 May 2024 doi:10.20944/preprints202405.1464.v1

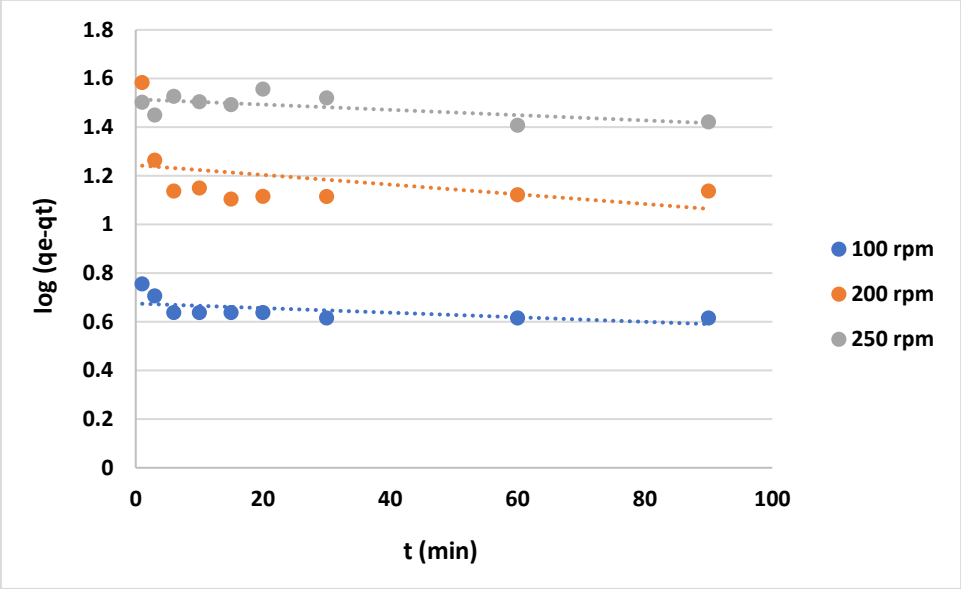

Figure 13. Plots of "pseudo-first-order model" for adsorption of MB on anionic CNF at different agitation speeds.

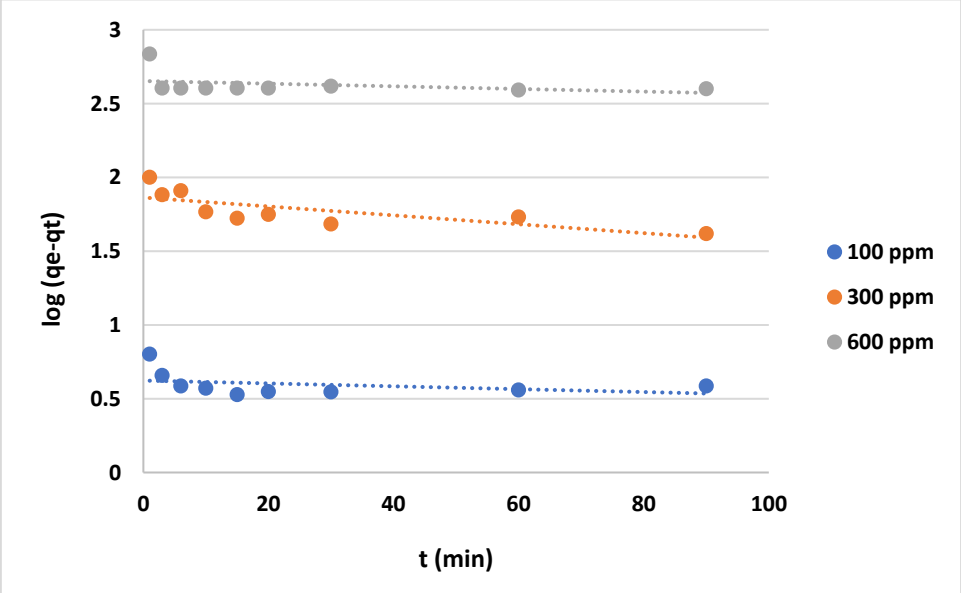

Figure 14. Plots of "pseudo-first-order model" for adsorption of MB on anionic CNF at different initial concentrations.

 doi:10.20944/preprints202405.1464.v1

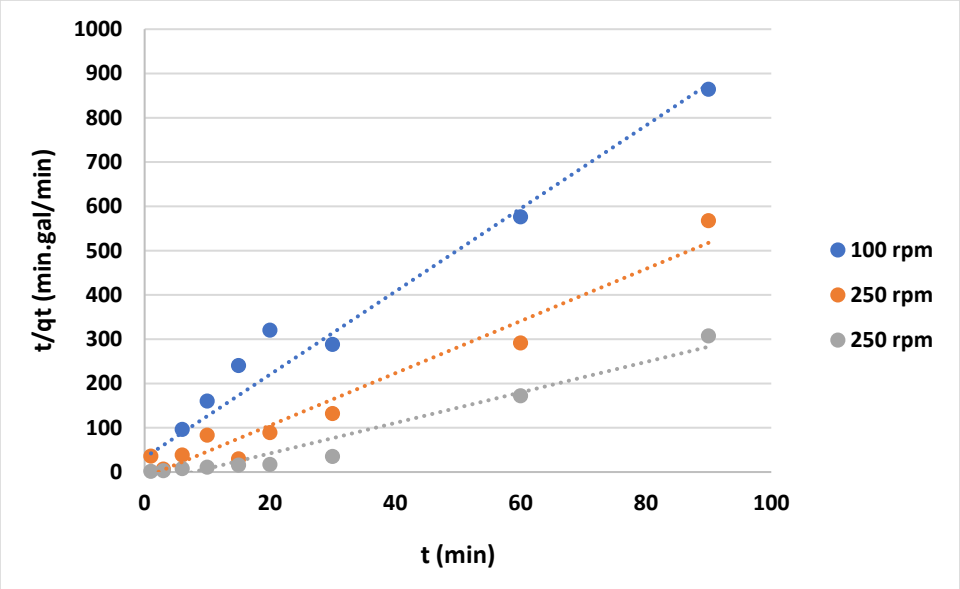

Figure 15. Graphs of the "pseudo-second-order model" for MB adsorption on anionic CNF at various agitation speeds.

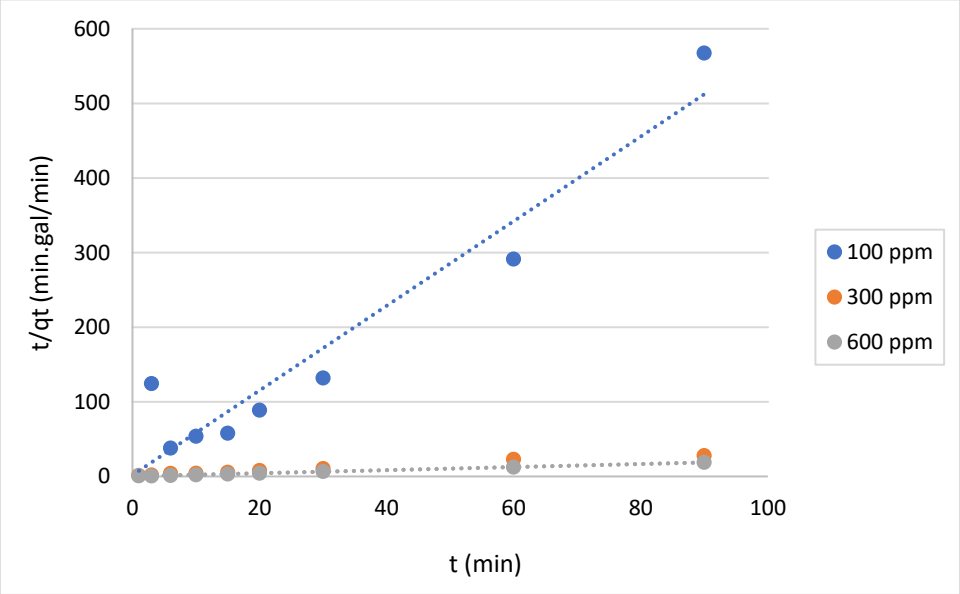

Figure 16. Graphs of the "pseudo-second-order model" for MB adsorption on anionic CNF at different initial concentrations.

Preprints.org (www.preprints.org) | NOT PEER-REVIEWED | Posted: 23 May 2024 doi:10.20944/preprints202405.1464.v1

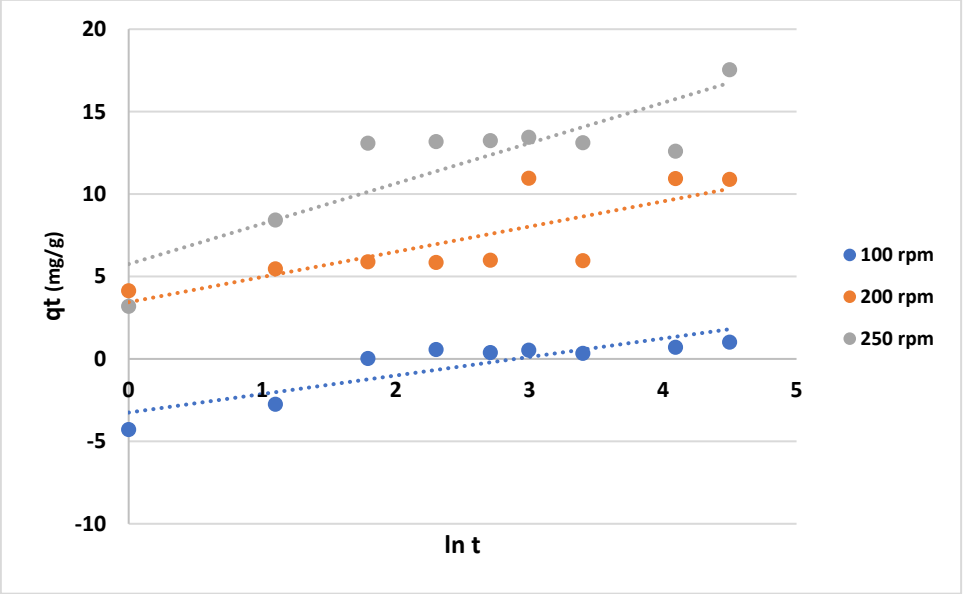

Figure 17. Plots of the "Elovich model" for adsorption of MB on anionic CNF at different agitation speeds.

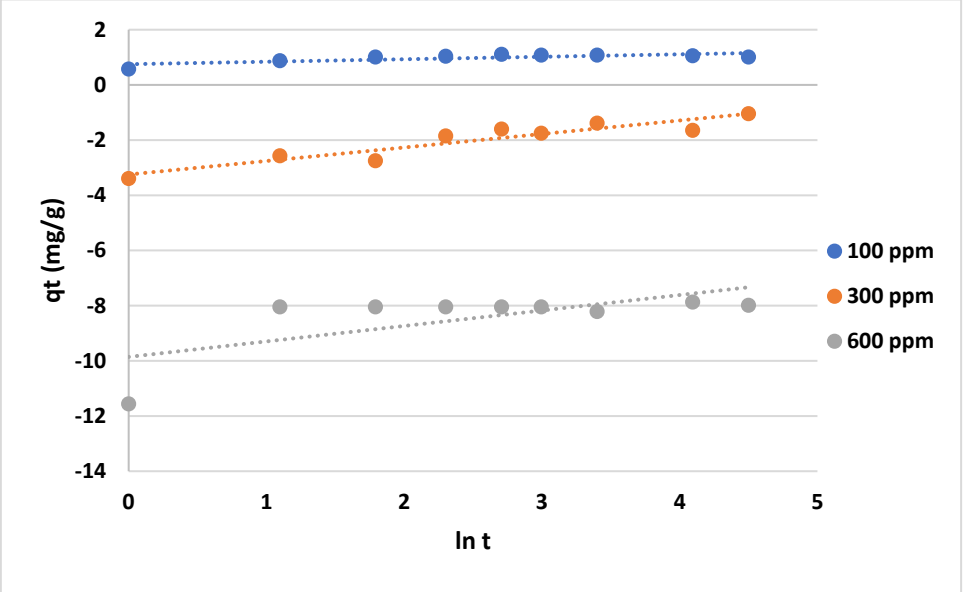

Figure 18. Plots of the "Elovich model" for adsorption of MB on anionic CNF at different initial concentrations.

3.8.2. Comparison between the Kinetic Models

As for mentioned, to ascertain the rate of the chemical reaction between MB and anionic CNF as the prime controlling step, the kinetic adsorption of MB on CNF was examined using a variety of models, including the pseudo-first-order, pseudo-second-order, and Elovich models. A statistical indicator of the linear relationship between two variables is the R^2. In comparison to the experimental values, the pseudo-first-order model's correlation coefficient R^2 was comparatively low, as demonstrated by the results. A low correlation coefficient suggests that there may be other unaccounted factors affecting the adsorption process. In contrast, the second-order equation fits well the experimental data. This suggests that the latter is more suitable for describing the adsorption kinetics of MB on CNF. This is further supported by the higher adsorption-rate constant (k_2) in the pseudo-second-order model, suggesting chemisorption as the rate-limiting step.

The findings from Gomaa et al. regarding MB adsorption on the CuO@BSS nanocomposite [48] and Fe^3+ adsorption on a hybrid spongy-like porous carbon material [49] reinforce the utility of the

Preprints.org (www.preprints.org) | NOT PEER-REVIEWED | Posted: 23 May 2024 doi:10.20944/preprints202405.1464.v1

pseudo-second-order kinetic model in describing adsorption processes that are likely controlled by chemisorption. The agreement of the maximum saturation capacity (qe) with experimental data further validates the model's applicability.

Aside from the above two models, elovich equation was also examined against the experimental data. The moderate fit of the Elovich model to the experimental data, indicated by rather higher R^2 values, suggests that it may also be a relevant model to describe the chemisorption process of MB on anionic CNF. The increase in the Elovich parameter β with agitation speed, while keeping the concentration constant, aligns with the expected decrease in available active sites, corroborating the findings of Gomaa et al. in their study of selective Fe^{3+} adsorption [49].

3.9. Adsorption Process Thermodynamics

There are several thermodynamic properties such as enthalpy (ΔH), the standard Gibbs free energy (ΔG), and the entropy (ΔS) changes, which are essential for understanding the nature of the adsorption process. It can explain the increase of the MB adsorption on anionic CNF with temperature elevated from 20°C to 60°C. The enthalpy change (ΔH) is calculated using the following equation [50]:

$$\ln K = \ln k_o + \left(\frac{-\Delta H}{R T}\right) \quad (16)$$

The enthalpy change (ΔH) can be determined by constructing a Van't Hoff plot, which is a graph of the natural logarithm of the equilibrium constant (ln K) versus the reciprocal of the absolute temperature (1/T) as shown in Figure 19 and also listed in Table 3. Meanwhile, The standard Gibbs free energy change (ΔG) is calculated using the Gibbs equation, which relates ΔG to the equilibrium constant (K), the gas constant (R), and the absolute temperature (T) [50]:

$$\Delta G = -R T \ln K \quad (17)$$

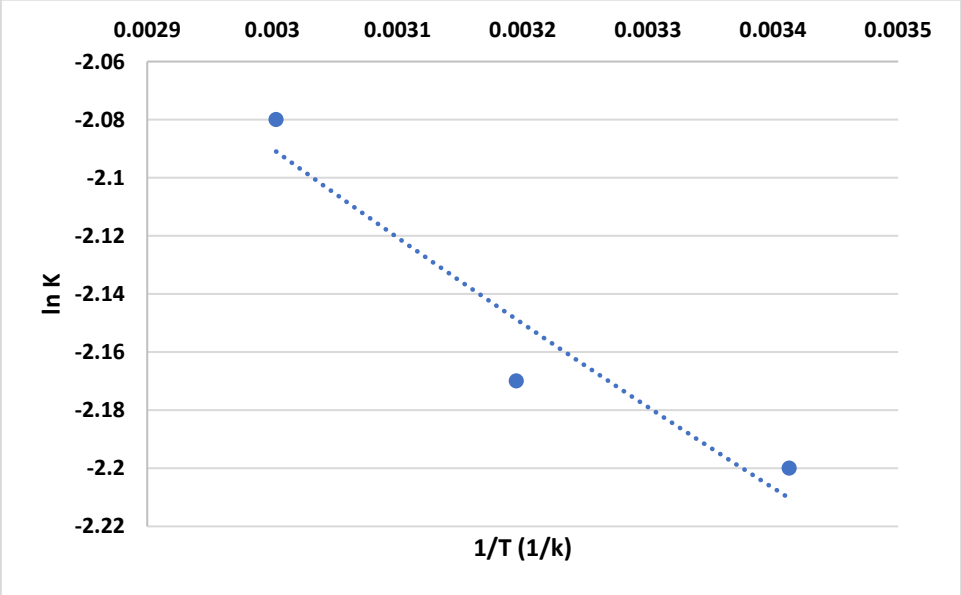

Figure 19. Relationship between ln K vs. 1/T.

Table 3. Thermodynamic parameters for the MB adsorption of anionic CNF at different temperature levels.

Temperature (°C)	ΔH (KJ/mol)	ΔG (KJ/mol)	ΔS (KJ/mol. K)
20		5.47	-0.0416
40	-6.71	5.56	-0.0392
60		5.69	-0.0373

 doi:10.20944/preprints202405.1464.v1

The equilibrium constant (K) can be dimensionless and is calculated using the ratio of the concentration of MB adsorbed by anionic CNF at equilibrium (Csm) to the concentration of MB in the solution at equilibrium (Cem), as expressed in equation (18) [51]:

$K = Cs_m/Ce_m$ (18)

Lastly, the entropy change (ΔS) is calculated using the Gibbs-Helmholtz equation, which relates ΔS to ΔH, ΔG, and T [50] as follows:

$$\Delta S = \left(\frac{\Delta H - \Delta G}{T} \right) \quad (19)$$

The negative values of ΔH indicate exothermic adsorption process. Hence increasing the temperature causes the increase of the MB adsorption on anionic CNF. The sign of ΔS can provide information about the disorder or randomness associated with the adsorption process. The negative values of ΔS, as shown in Table 3, typically indicate a decrease in disorder upon adsorption. It means the MB-anionic CNF adsorption process may be favorable [52]. The Gibbs equation is a fundamental equation in thermodynamics that provides insight into the spontaneity of a process. A positive ΔG indicates a non-spontaneous process under standard conditions.

3.10. Comparison of Waste Palm Leaves-Derived Anionic CNF as an Adsorbent with Literature-Reported Adsorbents

The utilization of agricultural waste such as palm leaves for the extraction of high-value materials like anionic CNF not only contributes to waste reduction but also offers a cost-effective alternative to traditional raw materials. The fact that the performance of anionic CNF derived from waste palm leaves is on par with other adsorbents mentioned in the literature (see Table 4) is a indication to the potential of this approach. It is encouraging to note that the local and inexpensive nature of the raw material does not detract from the efficacy of the product.

Table 4. A comparison of prepared anionic CNF with other reported literature results.

Ref	Adsorbent type	Solution	T (°C)	Capacity mg/g
[53]	CNF Membrane	Crystal Violet (CV)	25	4
[54]	CNF	Congo Red (CR)	25	6.6
This work	Anionic CNF	MB	25	4.25

4. Conclusions

Highly efficient bio-sorbent for MB dye; has been developed by extracting the cellulose pulp from the leaflet of a palm date tree and transferring it into nano–cellulose via multi-chemical treatment. The obtained nano-material shows significant dye removal performance. The temperature and pH are the significant parameters in the dye removal. Therefore, the adsorption process is endothermic, the maximum removal efficiency has been recognized at pH= 6 and temperature= 60°C. It was also found that the electrostatic changes of the solution resulting from the pH change greatly affect the dye removal. The electrostatic changes at the maximum capacity of the nano-cellulose in adsorption of the dye were 4.25 mg/g at room temperature.

Two equilibrium models, the Langmuir and Freundlich models were employed. The use of equilibrium models like Langmuir and Freundlich to describe the adsorption isotherms is a standard approach in adsorption studies. It is noteworthy that the Langmuir model, which assumes monolayer adsorption on a homogeneous surface with a finite number of identical sites, was consistent with the experimental data. This suggests that the adsorption sites on the anionic CNF are uniform and that each site binds to one dye molecule. The highest removal efficiency was obtained at 60°C and was 5 mg/g.

Kinetic studies involving various models such as pseudo-first-order, pseudo-second-order, and Elovich equations are crucial for understanding the dynamics of the adsorption process. The pseudo-second-order model fitting the experimental data well suggests that the rate-limiting step may be chemical adsorption involving valency forces through sharing or exchange of electrons between the adsorbent and the adsorbate. The Elovich equation further supports the chemical nature of the adsorption, indicating a reaction between the MB dye and the anionic CNF.

Overall, the study's findings contribute valuable insights into the potential use of renewable natural waste sources for environmental remediation, particularly in the removal of cationic contaminants. It also underscores the importance of understanding the adsorption kinetics and mechanism to optimize the process for practical applications. The use of anionic CNF from palm date leaves as an adsorbent is an innovative approach that combines sustainability with effective wastewater treatment.

Author Contributions: Conceptualization, F.F, M.H., S.A and A.G.; Methodology, F.F, A.K, M.A and M.H.; Software, M.A., A.G., MK; Validation, A.K., A.G., A.A and K.B.; Formal analysis, F.F, A.A. and M.H.; Investigation, A.K. and A.G., MK; Resources, A.K. and A.A., F.F; Data curation, A.A., MK and A.G..; Writing—original draft preparation, F.F., M.H., S.A and A.G; Writing—review and editing, All authors; Visualization, M.A, A.G, S.A. and F.F.; Supervision, S.A., M.H., M.A and K.B; Funding acquisition, S.A. and M.H. All authors have read and agreed to the published version of the manuscript.

Funding: This research received financial support of this work by the Deanship of Scientific Research at Imam Mohammad Ibn Saud Islamic University (IMSIU) for funding through Research Partnership No. IMSIU-RP23052.

Data Availability Statement: Data are contained within the article.

Acknowledgments: This research received financial support of this work by the Deanship of Scientific Research at Imam Mohammad Ibn Saud Islamic University (IMSIU) for funding through Research Partnership No. IMSIU-RP23052. Also, the authors appreciate and thank Imam Mohammad Ibn Saud Islamic University (IMSIU), King Abdulaziz City for Science and Technology (KACST, and National Research Centre (Egypt), for supporting this cooperative work with facilities that enable the research plan to commit its targets.

Conflicts of Interest: The authors declare that the research was conducted in the absence of any commercial or financial relationships that could be construed as a potential conflict of interest.

References

1. A. Al-Hyali, Emad, Omar M Ramadhan, and Safwan A Al-Dobone. "Effect of Substituents Type on the Adsorption of Aromatic Carboxylic Acids and their Relation to Concentration, Temperature and pH" Rafidain Journal of Science 16.8 (2005): 68-79.
2. Mona A. Abdel-Fatah, H. O. Sherif, Fatma Agour, and S. I. Hawash. "Textile Wastewater Treatment By Chemical Coagulation Technology", Global Journal of Advanced Engineering Tech and Sci, Vol. 2(12): pp 20-28, (2015)
3. Ahmed F. Shaaban, Azza I. Hafez, Mona A. Abdel-Fatah, Nabil M. Abdel-Monem, Mohamed Hanafy Mahmoud. "Process engineering optimization of Nanofiltration unit for the treatment of textile plant effluent in view of solution-diffusion model", Egyptian Journal of Petroleum, Vol. 25(1): pp 79–90, (2016) http://dx.doi.org/10.1016/j.ejpe.2015.03.018
4. Sell, Nancy J. Industrial pollution control: issues and techniques. John Wiley & Sons, 1992.
5. Sarkar, Shrabana, et al. "Degradation of synthetic azo dyes of textile industry: a sustainable approach using microbial enzymes." Water Conservation Science and Engineering 2.4 (2017): 121-131.
6. Anderson, Sally, Harry L. Anderson, and William Clegg. "Crystal structure of an azo dye rotaxane" Chemical Communications 21 (1998): 2379-2380.
7. O'Neil, M.J., "The Merck Index: An Encyclopedia of Chemicals, Drugs, and Biologicals". 14th ed. New Jersey: Merck, (2006)
8. Ahankari, Sandeep, et al. "Anionic CNF as a sustainable material for water purification". SPE Polymers 1.2 (2020): 69-80.
9. Lima, Eder C. "Removal of emerging contaminants from the environment by adsorption." Ecotoxicology and environmental safety 150 (2018): 1-17.
10. Bharathi, K. S., and S. T. Ramesh. "Removal of dyes using agricultural waste as low-cost adsorbents: a review." Applied Water Science 3.4 (2013): 773-790.

 doi:10.20944/preprints202405.1464.v1

11. Manzoor, Javid, and Manoj Sharma. "Impact of Textile Dyes on Human Health and Environment." Impact of Textile Dyes on Public Health and the Environment. IGI Global, (2020): 162-169.
12. Gajda, Sokolowska. "Synthetic dyes based on environmental considerations." Dyes Pigments 30 (1996): 1-20.
13. Mona A. Abdel-Fatah, E. M. H. Khater, A. I. Hafez, A. F. Shaaban. "Performance of Fouled NF Membrane as Used For Textile Dyeing Wastewater, Membrane Water Treatment", Techno-Press; Vol. 11(2), pp 111 - 121, (2020). https://doi.org/10.12989/mwt.2020.11.2.111
14. Kabdaşli, I., O. Tünay, and D. Orhon. "Wastewater control and management in a leather tanning district" Water science and technology 40.1 (1999): 261-267.
15. Bensalah, N., MA Quiroz Alfaro, and C. A. Martínez-Huitle. "Electrochemical treatment of synthetic wastewaters containing Alphazurine A dye." Chemical Engineering Journal 149.1-3 (2009): 348-352.
16. Wróbel, Danuta, Andrzej Boguta, and Rodica M. Ion. "Mixtures of synthetic organic dyes in a photoelectrochemical cell." Journal of Photochemistry and Photobiology A: Chemistry 138.1 (2001): 7-22.
17. Dawood, Sara, Tushar Kanti Sen, and Chi Phan. "Synthesis and characterization of novel-activated carbon from waste biomass pine cone and its application in the removal of congo red dye from aqueous solution by adsorption." Water, Air, & Soil Pollution 225.1 (2014): 1-16.
18. Norrrahim, Mohd Nor Faiz, et al. "Anionic cellulose nanofiber (CNF): a bioadsorbent for chemical contaminant remediation." RSC Advances 11.13 (2021): 7347-7368.
19. Sarici-Özdemir, Çiğdem, and Yunus Önal. "Study to observe the applicability of the adsorption isotherms used for the adsorption of medicine organics onto activated carbon." Particulate Science and Technology 36.2 (2018): 254-261.
20. de Franco, Marcela Andrea Espina, et al. "Diclofenac removal from water by adsorption using activated carbon in batch mode and fixed-bed column: isotherms, thermodynamic study and breakthrough curves modeling." Journal of Cleaner Production 181 (2018): 145-154.
21. Mona A. Abdel-Fatah, Ahmed Abd El Maguid, and Ashraf Amin. "Studying the Oxygen Requirement for Aeration Systems in Wastewater Treatment Plants", ARPN Journal of Engineering and Applied Sciences, Vol. 16(9): pp 947-952, (2021)
22. Guedidi, Hanen, et al. "Adsorption of ibuprofen from aqueous solution on chemically surface-modified activated carbon cloths." Arabian Journal of Chemistry, 10 (2017): S3584-S3594.
23. Fröhlich, A. C., et al. "Three-dimensional mass transfer modeling of ibuprofen adsorption on activated carbon prepared by sonication." Chemical Engineering Journal, 341 (2018): 65-74.
24. Li, Zichao, et al. "Adsorption of congo red and methylene blue dyes on an ashitaba waste and a walnut shell-based activated carbon from aqueous solutions: Experiments, characterization and physical interpretations." Chemical Engineering Journal 388 (2020): 124263.
25. Joshi, Pratiksha, et al. "Fruit Waste-Derived Cellulose and Graphene-Based Aerogels: Plausible Adsorption Pathways for Fast and Efficient Removal of Organic Dyes." Journal of Colloid and Interface Science (2021).
26. Javanbakht, Vahid, and Zahra Rafiee. "Fibrous polyester sponge modified with carboxymethyl cellulose and Zeolitic imidazolate frameworks for methylene blue dye removal in batch and continuous adsorption processes." Journal of Molecular Structure 1249 (2022): 131552.
27. Wang, Shuai, et al. "Efficient and selective adsorption of cationic dyes with regenerated cellulose." Chemical Physics Letters 784 (2021): 139104.
28. Li, Yuchen, et al. "Redox-responsive carboxymethyl cellulose hydrogel for adsorption and controlled release of dye." European Polymer Journal 123 (2020): 109447.
29. Hasan, I.; El-Din, S.; AbdElRaady, A. "Peppermint-Mediated Green Synthesis of Nano ZrO_2 and Its Adsorptive Removal of Cobalt from Water". Inorganics 10 (2022): 257–273.
30. Gad, H.; Omar, H.; Aziz, M.; Hassan, M.; Khalil, M. "Treatment of Rice Husk Ash to Improve Adsorption Capacity of Cobalt from Aqueous Solution". Asian J. Chem. 28 (2016): 385–394.
31. Swelam, A.; Salem, A.; Ayman, A.; Farghly, A. "Kinetic and Thermodynamic Sorption Study of Cobalt Removal from Water Solution with Magnetic Nano-Hydroxyapatite". Al Azhar Bull. Sci. (2018) 29, 45–58.
32. Gh. Al Bazedi, Ehab Abadir, Mona A. Abdel-Fatah. "Treatment of Blue HB Reactive Dyes in Textile Wastewater using Bio-waste based Hydroxyapatite", Egyptian Journal of Chemistry, Vol. 65(5): pp 23-31, (2022). https://doi.org/10.21608/ejchem.2022.115407.5234
33. Gomaa, H.; Hussein, M.A.; Motawea, M.M.; Aboraia, A.M.; Cheira, M.F.; Alotaibi, M.T.; El-Bahy, S.M.; Ali, H.M. "A hybrid mesoporous CuO@barley straw-derived SiO_2 nanocomposite for adsorption and photocatalytic degradation of methylene blue from real wastewater". Colloids Surf. A Physicochem. Eng. Asp. (2022) 644, 128811.
34. Gomaa, H.; Sayed, A.; Mahross, M.; Mohamed, A.; Ismail, M.; Othman, A.; Jiansheng, B.; El-Bahy, M. A hybrid spongy-like porous carbon-based on azopyrazole-benzene-sulfonamide derivative for highly selective $Fe3^{+}$-adsorption from real water samples. Microporous Mesoporous Mater. (2022), 330, 111578.

35. Gomaa, H.; El-Monaem, E.; Eltaweil, A.; Omer, A. Efcient removal of noxious methylene blue and crystal violet dyes at neutral conditions by reusable montmorillonite/ $NiFe_2O_4$@amine-functionalized chitosan composite. Sci. Rep. (2022) 12, 15499.
36. Kassem, K.; Hussein, M.; Motawea, M.; Alrowaili, Z.; Ezzeldien, M. Design of mesoporous ZnO @ silica fume-derived SiO_2 nanocomposite as photocatalyst for efficient crystal violet removal: Effective route to recycle industrial waste. J. Clean. Prod. (2021) 326, 129416.
37. Salama, R.; El-Hakam, S.; Samra, S.; El-Dafrawy, S.; Ibrahim, A.; Ahmed, A. "Synthesis, characterization of titania supported on mesoporous MCM-41 and its application for the removal of methylene blue". Delta Univ. Sci. J. (2022) 5, 321–339.
38. Wenjie Dong, Xiaorong Gu, Yu Shu1, Dingyi Cao, Jingyi Yu, Mona A. Abdel-Fatah, Hailu Fu, Pulse electrocoagulation combined with a coagulant to remove antimony in wastewater, Journal of Water Process Engineering, Vol 47, June (2022), 102749, https://doi.org/10.1016/j.jwpe.2022.102749
39. Hailu Fu, Lingling Zhong, Ziyao Yu, Wenxiang Liu, Mona A. Abdel-Fatah, Jinye Li, Mingzhang, Jie Yu, Wenjie Dong, Sang Soo, Lee; Enhanced adsorptive removal of ammonium on the Na^+/Al_3^+ enriched natural zeolite, Separation and Purification Technology, Volume 298, (2022) 121507
40. J. C. C. S, N. George, and S. K. Narayanankutty, "Isolation and characterization of cellulose nanofibrils from arecanut husk fibre". Carbohydr. Polym., vol. 142, pp. 158–166, (2016)
41. Sharma, P.R.; Chattopadhyay, A.; Sharma, S.K.; Hsiao, B.S. "Efficient Removal of UO_2^{2+} from Water Using Carboxy-cellulose Nanofibers Prepared by the Nitro-Oxidation Method". Ind. Eng. Chem. Res. (2017) 56, 13885–13893.
42. Mona A. Abdel-Fatah, Marwa M. Elsayed; "Electrochemical Techniques Applied for Industrial Wastewater Treatment: A Review", Egyptian Journal of Chemistry, Vol. 67(4): pp 7-33, (2024)
43. Mona A. Abdel-Fatah, Gh. Al Bazedi, Ashraf Amin. "Optimization of Nickel Catalyst Loading in $Ni/\gamma Al_2O_3$ for Producing Carbon Nanotubes through Natural Gas Decomposition", Chemical Papers, Springer Nature, (2023) https://doi.org/10.1007/s11696-023-02737-z
44. EL-Geundi, M. Adsorption Equilibria of Basic Dyestuffs onto Maize Cob. Adsorp. Sci. and Technol. (1990), 7, 114.
45. Suresh, S.; Srivastava, V.; Mishra, I. "Study of Catechol and Resorcinol Adsorption Mechanism through Granular Activated Carbon Characterization, pH and Kinetic Study". Sep. Sci. Technol. Sep. Sci. Technol. (2011) 46, 1750–1766.
46. Demirbaş, E. "Adsorption of cobalt (II) ions from aqueous solution onto activated carbon prepared from hazelnut shells". Adsorpt. Sci. Technol. (2003) 21, 951–963.
47. Mckay, G.; Ho, S. "Application of kinetic models to the sorption of copper (II) on to peat". Adsorpt. Sci. Technol. (2002) 20, 797.
48. Gomaa, H.; Hussein, M.A.; Motawea, M.M.; Aboraia, A.M.; Cheira, M.F.; Alotaibi, M.T.; El-Bahy, S.M.; Ali, H.M. "A hybrid mesoporous CuO@barley straw-derived SiO_2 nanocomposite for adsorption and photocatalytic degradation of methylene blue from real wastewater". Colloids Surf. A Physicochem. Eng. Asp. (2022) 644, 128811.
49. Gomaa, H.; Sayed, A.; Mahross, M.; Mohamed, A.; Ismail, M.; Othman, A.; Jiansheng, B.; El-Bahy, M. A "hybrid spongy-like porous carbon-based on azopyrazole-benzene-sulfonamide derivative for highly selective Fe^{3+}-adsorption from real water samples". Microporous Mesoporous Mater. (2022) 330, 111578.
50. Ruixia, W., Jinlong, C., Lianlong, C., Zheng-hao, F., Ai-min, L., Quanxing, Z. "Study of the Adsorption Thermodynamics and Kinetics of Lipoic Acid onto Three Types". Adsorp. Sci. Technol., 22, 523. (2014)
51. Namasivayam, C., Ranganathan, K. (1994) Recycling of 'waste' FE(III) /CR(III) hydroxide for the removal of nickel from wastewater: Adsorption and equilibrium studies, Waste Manag., 14, 709.
52. Banat, F., Al-Asheh, S., Rousan, D. (2002) A Comparative of Copper and Zinc Ion Adsorption on to Activated and Non-activated Date-Pits, Adsorp. Sci.Technol., 20, 319.
53. Ma, H., Burger, C., Hsiao, B. S., & Chu, B. (2012). Nanofibrous Microfiltration Membrane Based on Cellulose Nanowhiskers. Biomacromolecules, 13(1), 180–186. https://doi.org/10.1021/bm201421g
54. Zhang, L., Huo, X., Zhu, J., Liu, C., & Wang, L. (2023). "Residual Chlorella-Based Cellulose Nanofibers and Their Quaternization Modification and Efficient Anionic Dye Adsorption". Materials, 16(10).